

Antonio GARCIA<sup>1</sup>, Tim GUST<sup>1</sup>, Enes BASATA<sup>1</sup>, Tim GERSTING<sup>1</sup>,  
Michal DEKA<sup>1</sup>, Sven THIELE<sup>1</sup>, Mohammad SALAH<sup>1</sup>,  
Matias Bestard KOERNER<sup>2</sup>, Torben RUNTE<sup>3</sup>, Miguel GONZALEZ<sup>3</sup>

## VIBES: Visionary Ingenuity Boosting European Spacecraft. Managing microvibrations for the future of spaceflight

**Received** 6 November 2022, **Revised** 31 December 2022, **Accepted** 3 February 2023, **Published online** 30 March 2023

**Keywords:** microvibrations, isolation, satellite architectures, metrology, control

Microvibrations are mechanical oscillations caused by components such as the reaction wheels of an attitude control system of a spacecraft. These microvibrations are transferred through the spacecraft structure onto important instruments (e.g., optical instruments), causing those to produce diminished results (e.g., reduced image quality, imprecise geolocation etc.). At the present state, microvibrations in spacecraft cannot be actively controlled because their very high frequencies of up to 1000 Hz are above the control bandwidth a current attitude control system can provide. However, being able to reduce the effects of microvibrations on a space mission is becoming increasingly more critical as the envelope of future optical satellite missions expands. Furthermore, the advancements made in the performance of small satellites as well as the growing interest in laser and quantum communication call for a cost-efficient solution for managing microvibrations. This paper describes how cheap MEMS-based measurement systems have already proven that they are a potential solution. Showing high sensitivity and low-noise performance while allowing fast and easy prototyping.

---

✉ Antonio Garcia, email: [antonio.garcia@hs-bremen.de](mailto:antonio.garcia@hs-bremen.de)

<sup>1</sup>City University of Applied Sciences Bremen, Institute of Aerospace Technologies, Bremen, Germany

<sup>2</sup>German Aerospace Center – DLR, Institute of Space Systems. Guidance, Navigation and Control Systems. Bremen, Germany

<sup>3</sup>OHB System AG, Bremen, Germany



© 2023. The Author(s). This is an open-access article distributed under the terms of the Creative Commons Attribution (CC-BY 4.0, <https://creativecommons.org/licenses/by/4.0/>), which permits use, distribution, and reproduction in any medium, provided that the author and source are cited.

## 1. Introduction: Microvibration Engineering until now and the VIBES-Approach

There are multiple common approaches to predicting, analyzing and counteracting microvibrations, many of which are described in the ECSS Handbook on the mechanical load analysis of spacecraft [1]. On missions with an extended budget such as large space observatories, the workflow might consist of a pre-build analysis using a complete finite-element-model of the spacecraft to identify modes of resonance of the entire structure and subsequent analytical calculations based on the obtained transfer functions. Then, these results are experimentally verified by measuring the mechanical response of the physical spacecraft in in-orbit condition on the ground. These methods work, however, they are not only expensive due to extensive pre-launch testing campaigns but can also cause unexpected problems during the mission, as the spacecraft can react very differently to mechanical excitations during operation in space, e.g., in the case of the Chandra X-ray space telescope [2].

Additional software-driven tools of microvibration engineering as described by [3] can optimize existing workflows by improving the evaluation of results from classical methods. The main sources of microvibrations are attitude-control-system components of the spacecraft such as reaction wheels, which is the reason why studying them as a perturbation source is important [4, 5]

Microvibrations are a critical issue for many past, ongoing and future missions [6] with a wide range of countermeasures that are mostly mission specific and have to be developed in a lengthy and costly process, thus making low-budget missions with a high criticality of microvibrations not very feasible.

This is what the team of the VIBES project is currently trying to change: at the Institute of Aerospace Technologies (IAT) of the City University of Applied Sciences Bremen in collaboration with DLR and OHB System a testbed is being set-up on which the different sensors for the measurement of microvibrations as well as passive and active control systems can be tested and compared. The eventual goal is to develop different systems that are capable of actively managing the microvibrations in a small spacecraft.

Fig. 1 shows a conceptual spacecraft where the mentioned elements of the project are depicted: a vibration source such as reaction wheel is mounted on the spacecraft structure. Passive and active microvibration isolation systems are used at the relevant mechanical interfaces to minimize the influence on the optical payload. Additionally, an Active Pointing System will stabilize the line of sight of the payload. The contribution of each element to the final optical quality of the measured reference scene shall be analyzed. On the right-hand side of Fig. 1 the CAD design of the testbed is shown. It consists of a mechanically decoupled suspension where a satellite structure will be placed containing vibration sources such as reaction wheels, passive and active isolation systems and an optical payload.

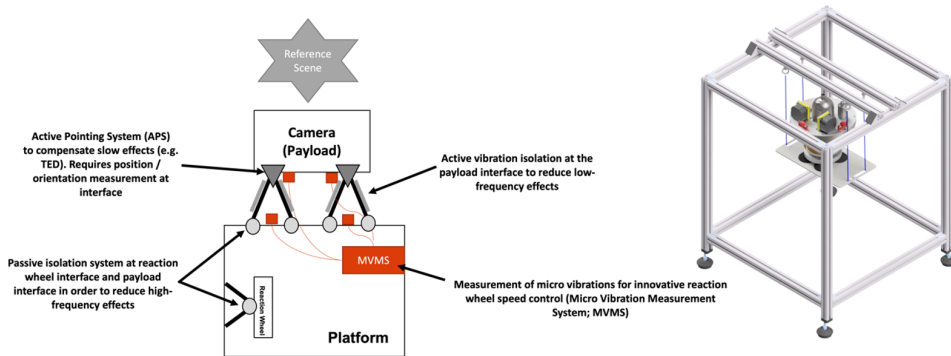


Fig. 1. Left: Overview of the VIBES microvibrations products and technologies that will be developed to improve in orbit satellite performance. Right: CAD Design of the satellite testbed where the VIBES elements will be developed and tested. It consists of a mechanically isolated platform for a satellite structure containing all the elements of the sketch on the left-hand side

This paper summarizes the current status of the VIBES microvibration project, which started in summer 2021 and is based on an incremental development approach. The current microvibration source is the shaker described in Section 2, which allows verification of the testbed via controlled injection of forces before we move to reaction wheels. The shaker is used as input to the microvibration measurement system (MVMS) in the laboratory, as discussed Section 3. Using the Data Analysis Tools presented in Section 4, the MVMS has been used to characterize the mechanical suspension of the testbed as presented in Section 5. The Section 6 shows ongoing development steps: implementation of vibration control systems and wireless implementation of the MVMS.

## 2. Microvibration source: shaker with inertial mass actuators as verification strategy

One of the steps in the development and operation of the testbed is the verification of the testbed design using reference input forcing functions in the form of vibrations, e.g., replicating those caused by a piece of equipment during operation. The generated vibrations serve the identification of the testbed's normal modes and the identification of optimal points to mount equipment. Specifically, these points may be appropriate because the impact of the vibrations of the mounted equipment onto the testbed is either maximized or minimized. Once the testbed is identified, the vibrations serve as a reference input for the payloads and sensors mounted onto the testbed and hence provide comparability among different setups.

While practical, using spacecraft components, such as reaction wheels, to generate reference vibrations is limited in the frequencies and amplitudes they generate. The testbed instead can use a shaker with actuators that can generate forces and torques at a constant amplitude over a wide band for the characterization

and verification using reference vibrations. Furthermore, it may be of interest for certain applications to be able to replicate specific input forcing function envelopes previously recorded. Satellites in orbit are to be considered free-free systems, with no larger inertial mass attached or moving through a fluid. This means that the testbed itself will have to replicate this condition, in this case being decoupled from the laboratory and the building. Accordingly, these conditions apply to the shaker and have to be considered to achieve a flexible and reconfigurable design. The solution implemented uses a shaker based on inertial actuators which accelerate a mass to generate inertial forces mounted directly on the testbed without an interface to the laboratory floor.

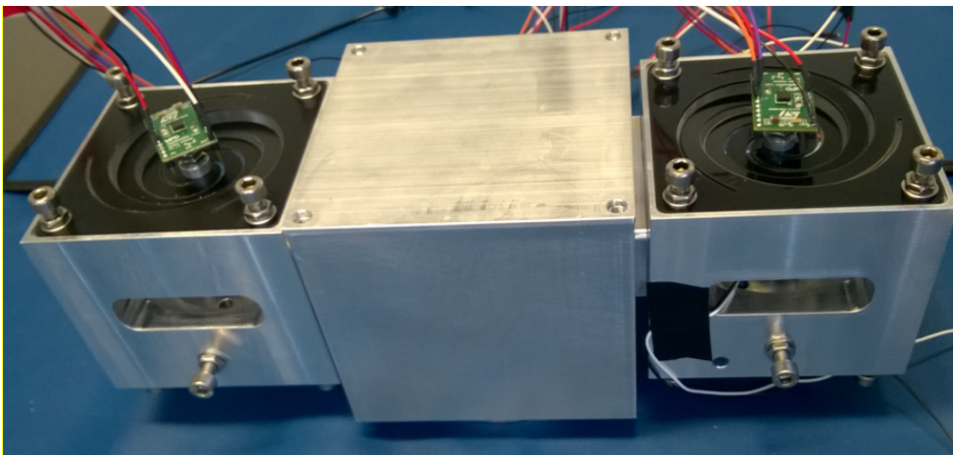


Fig. 2. Shaker with two VCAs mounted vertically on the left and right and each with a reference accelerometer (green) mounted on the inertial masses integrated onto springs (black)

The testbed is equipped with a shaker that uses a pair of Voice Coil Actuators (VCA) taking advantage of its direct drive configuration to generate forces and torques proportional to an input current with the movable part of the actuator serving as the inertial mass. VCAs are available as Commercial off-the-shelf Components (COTS) in a wide range of designs, allowing an easy scalability in terms of operation forces, frequency bands and dimensions. The selected VCAs use springs as bearings to keep the movable part of the actuator aligned and provide a resettling point if powered off, hence not requiring movable mechanisms to operate which may introduce unwanted noise onto the testbed.

The VCAs are arranged in as a pair around a central axis, meaning that the actuators can generate from linear forces to a net torque depending on the phase shift between the input signal given to them. The interface between the two actuators has been designed to allow a high usable bandwidth between 10 Hz and 1000 Hz, but the structural response of the mounting point has to be considered and adapted for the specific testcase. The shaker is suited for a constant operation with a force

amplitude of 0.5 N per VCA over the full bandwidth and has a lever arm of 96 mm from the central axis.

The shaker uses a pre-amplifier and a power amplifier to drive the VCAs proportionally to an input or reference signal given. The source of the input signal can be either a laboratory signal generator or a pre-recorded pattern to be reproduced. Analog accelerometers are mounted on the movable part of each VCA, being these the inertial masses, and provide feedback for the closed loop operation of the shaker if desired. Additional accelerometers or sensors like load cells can be integrated next to or in between the interface of the shaker and the testbed to provide information on the harmonic response of the testbed. The shaker electronics can be paired with an embedded system or real-time control computer to expand the capabilities of the testbed, including active vibration control. This approach is described in Subsection 6.1.

### 3. Microvibration measurement system MVMS

The main MVMS requirements have been iterated with industry and focus has been set on a cost and size optimized solution, to allow fast development cycles and potential implementation in future satellites with low resources impact. This system can also be used in the ongoing student satellite project AQUACUBE and the student rocket project AQUASONIC III at the IAT.

In this sense, the goal is to use MEMS sensors for the accelerometers and cost optimized microprocessors for the readout, that can be also used for the control strategies of reaction wheels and active line of sight in the future, as shown in the next sections. The complete system of accelerometers and readout electronics is then verified using a shaker with amplitudes comparable to that of satellite reaction wheels and significant SNR is demonstrated with measurement times in the order of seconds. This fulfills the needs of future experiments at satellite level, where the reactions wheels are expected to keep a constant rotation speed in this time frame.

#### 3.1. Evaluation and Selection of Micro Controllers and Control Systems

Table 1 below shows a comparison of two microcontrollers ESP32 and STM32 together with the PYNQ-Z2 board containing the system on-chip connecting the FPGA with the ARM processor. The PYNQ-Z2 board shown in Fig. 3 has not been fully verified so far in the project since it was recently acquired. Nevertheless, it will be used in the future due to superior performance and synergies with other projects at the IAT such as enabling the implementation of a software-defined radio for data transmission. Comparing the ESP32 and STM32 microcontrollers, the superiority of STM32 is visible in performance, however, ESP32 is still used in the project due to the easy and fast prototyping until a solution using the PYNQ-Z2 board is fully implemented.

Table 1. Relevant parameters taken into consideration for the market survey and pre-selected microprocessors for final evaluation. The PYNQ-Z2 board has been finally chosen for future implementation. Some measurements shown in this paper are still performed with STM32 or ESP32

Board	NUCLEO-H745ZI-Q	Adafruit HUZZAH32 ESP32 Feather Board	PYNQ-Z2
Processor	STM32H745ZIT6 Dual Core: 32-bit Arm Cortex-M7 480 MHz & 32-bit Arm Cortex-M4 240 MHz	240 MHz dual core Tensilica L	650 MHz dual-core Cortex-A9
Performance	1027 DMIPS and 300 DMIPS	300 DMIPS (one core)	1625 DMIPS (one core)
Memory	2 MB Flash, 1 MB RAM	520 KB SRAM, 4 MB Flash	512 MB DDR3, 16 MB Flash, MicroSD Slot
DA Converter	2x	2x	–
Power	USB or 3.3 V	USB or 3.3 V	USB or 7 V–15 V
Programmable Logic	–	–	13300 logic slices, 630 KB RAM

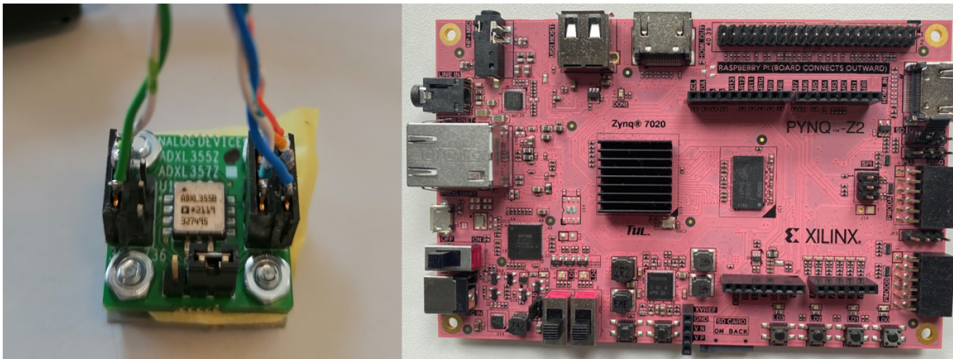


Fig. 3. Left: Selected MEMS accelerometer evaluation board. Size 6×6 mm. Right: Selected Microprocessor board PYNQ-Z2. Size 10×5 cm

### 3.2. Evaluation and selection of MEMS accelerometers

After a thorough market survey using the relevant parameters listed in the first column of Table 2, the sensors summarized in columns 2 to 4 have been pre-selected and subject to final evaluation.

To determine which model of MEMS accelerometer to use for further studies of microvibrations in the test setup, several parameters had to be taken into consideration. These parameters were first extracted from the respective datasheets and then verified experimentally. The ADXL355 sensor was chosen as it provides the best theoretical values of all three tested sensors and performed the best in



Table 2. Relevant parameters taken into consideration for the market survey and pre-selected MEMS accelerometers for final evaluation. The ADXL355 sensor has been finally chosen

Parameter	ADXL355	SEN17871	LIS3DH
Dimensions	6 mm×6 mm	2 mm×2 mm	3 mm×3 mm
Sensing Range	$\pm 2 \text{ g} \pm 4 \text{ g} \pm 8 \text{ g}$	$\pm 2 \text{ g} \pm 4 \text{ g} \pm 8 \text{ g} \pm 16 \text{ g}$	$\pm 2 \text{ g} \pm 4 \text{ g} \pm 8 \text{ g} \pm 16 \text{ g}$
Sensitivity	256000 LSB/g @ $\pm 2 \text{ g}$	16384 LSB/g @ $\pm 2 \text{ g}$	1000 LSB/g @ $\pm 2 \text{ g}$
Resolution	20 bit	16 bit	16 bit
Sampling Frequency	4 kHz	25 kHz (1.2 kHz)	5.3 kHz
Interface	SPI up to 10 MHz I <sup>2</sup> C up to 3.4 MHz	SPI up to 10 MHz I <sup>2</sup> C up to 3.4 MHz	SPI up to 10 MHz I <sup>2</sup> C up to 400 kHz
Voltage	3.3 V	3.3 V	3.3 V
Noise Density	22.5 $\mu\text{g}/\sqrt{\text{Hz}}$ @500 Hz	130 $\mu\text{g}/\sqrt{\text{Hz}}$ @50 Hz	220 $\mu\text{g}/\sqrt{\text{Hz}}$ @1.3 kHz

tests. The LIS3DH sensor is a cheap and available sensor and the SEN17871 has the highest sampling frequency, however, both either had lower expected values to begin with or under-performed in practice. Important parameters for the selection of the right MEMS device where the Noise Density and the Sensitivity as these values directly determine the lower limit of detectable vibrations. The sampling frequency is important when trying to measure high frequency oscillations, as the highest visible frequency will be the half of the sampling frequency. Although the ADXL355 has the lowest sampling frequency, 4 kHz will still be sufficient to comfortably measure vibrations close to 2 kHz.

To verify the actual performance of the sensors, extended experiments were conducted using the voice coil shaker with variable frequency input described in detail in Section 2. The device under test (DUT) was mounted to the shaker rigidly and set in motion while recording the data through an ESP32 microcontroller with an SPI link, as described in the Subsection 3.1. After data acquisition was finished, the obtained files were processed using internally developed software described in Section 4. The resulting visualizations were then used to interpret the measurements and verify both the sensors and the test setup.

Fig. 4 illustrates the measured acceleration of the ADXL355 sensor at rest over a 60-second-long period. The offset of 1 g was subtracted to make the comparatively small deviations easier to see. Since the ideal value would be a flat line of 0 m/s<sup>2</sup>, all deviation from 0 g can be interpreted as noise. Therefore, the standard deviation of the signal is equivalent to the RMS noise of the DUT [7]. The black dotted line represents the 1- $\sigma$  deviation, and the red dotted line shows the expected value under optimal conditions as calculated from the datasheet. It can be observed that the measured noise exceeds the expected noise by a factor of 1.79 or 2.1 mg in absolute acceleration. This meets the expectations because the test setup was not optimal and the only ODR of the DUT was higher than the baseline value for the datasheet's noise density.

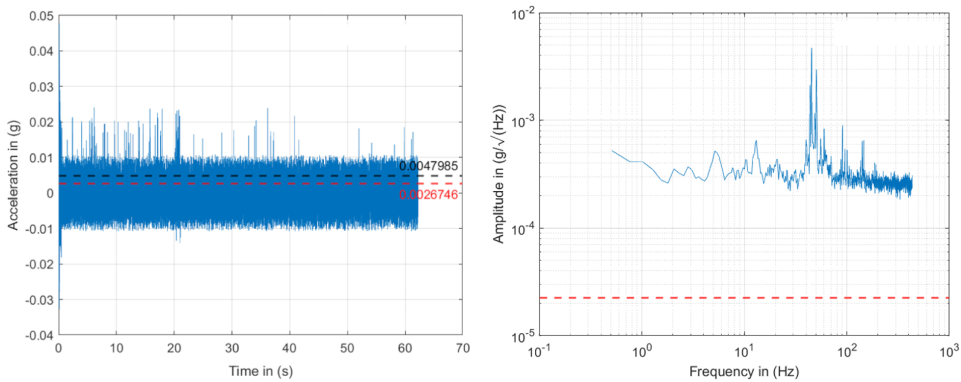


Fig. 4. Left: Time series of the MEMS accelerometer at rest. The red and black lines show the expected and measured RMS noise. Right: Corresponding Linear Spectral Density of the same measurement. The red line shows the noise level according to the data sheet

For a more direct comparison of noise levels and distributions of noise across the spectrum, a linear spectral density diagram was created. The noise density obtained from this calculation is also higher than the sensor's expected value and the distribution of the power across the frequency bandwidth is almost flat. This stands in accordance with the assumption that the noise of the sensor is Gaussian. The notable peak at approximately 50 Hz was likely caused by grid interference due to a non-optimal setup of the test. These factors will be eliminated in the future as the employed methods improve. In further experiments, the focus will be to closely match the expected characteristics and eliminate extrinsic noise and interference to more accurately determine parameters such as smallest detectable vibrations and shortest measurement-time to sense burst vibrations with acceptable signal-to-noise ratio.

#### 4. Software Tools for Data Analysis

The goal of the data processing is to develop a tool to quickly analyze and display the data measured by the STM32 or the ESP32.

The ability to analyze the data immediately is important because it is necessary to quickly assess whether an error occurred. If an error is noticed before a change of the test setup, the error can be fixed, and the measurement can be redone.

A dedicated application is coded to allow the immediate readout and analysis by everyone involved in the project, even without extensive programming or data analysis expertise. The Graphical User Interface of the application can be seen in Fig. 5.

The application allows the user to load multiple datasets, define the scope of the x-axis, change in which acceleration axis the analysis takes place and change multiple measurement system related options. The results are presented in multiple



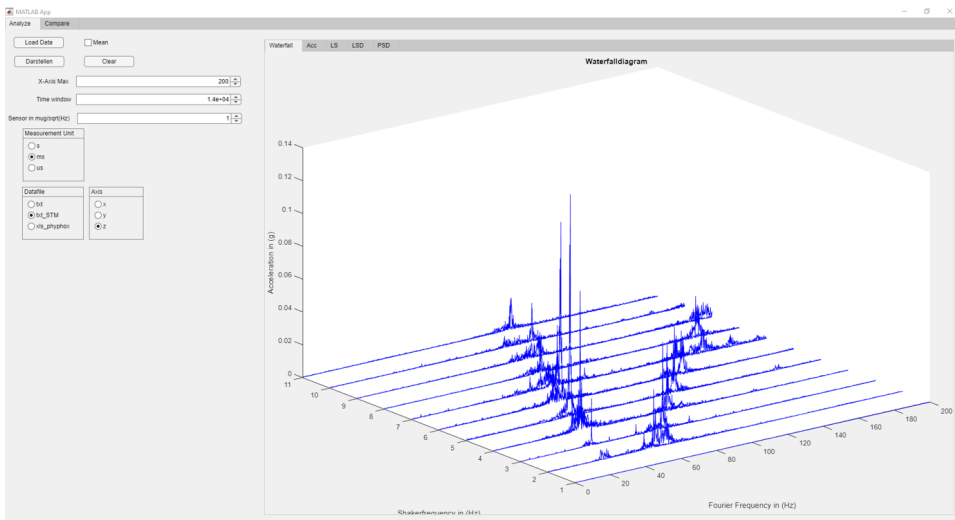


Fig. 5. Graphical User Interface of the data analysis toolbox showing a waterfall diagram for mechanical characterization of a vibration source, in this case the shaker described in Section 2. The X-axis shows the Fourier Frequency, the Y-Axis shows the different spectra where the shaker is operated at increasing revolutions and the Z-axis shows the spectral amplitude of the vibrations at different frequencies and operational set-points. The result show a first resonance at the operational frequency as well as a second harmonic response

different plots. The first one is a Waterfall plot, where the linear spectrum of each loaded measurement is shown.

In the acceleration tab, the acceleration data of each measurement is shown in the time and the frequency domain, as shown in Fig. 4. To get the linear spectrum, the data which is gathered in the time domain is transferred into the frequency domain using a Fast Fourier Transformation (FFT). In the linear spectrum, the exact frequency and amplitude of the frequency of the signal can be obtained.

Using the Linear Spectral Density (LSD) and the Power Spectral Density (PSD) the noise of the recorded data is examined so that a statement about the noise in the measurement can be made [8]. For all information that needs to be provided quickly, the application has proven to be beneficial. However, for a more specific examination of the data, specific analysis scripts are coded. Such scripts are used in the next section to evaluate the acceleration at different positions of the testbed.

## 5. The testbed set-up and evaluation of mechanical isolation

The current implementation of the testbed can be seen in Fig. 6. It is based on the CAD design presented in Fig. 1 and VIBES mechanical engineering division provides test setups required for data acquisition and develops mechanical interfaces such as 3D-printed parts to integrate the sensors and microcontrollers needed into

different test configurations. However, the core part is advancing the development of the test stand. Based on a previous bachelor's thesis, it uses steel springs to isolate a test plate from external vibration sources such as people walking in the laboratory [9]. To determine the degree of isolation achieved by the test stand, a series of measurements is performed with the MVMS. For these measurements, a compressor next to a corner of the test stand is used as vibration source and the test stand is configured with metal feet screwed into the four bottom corners. The test setup is shown in Fig. 6.

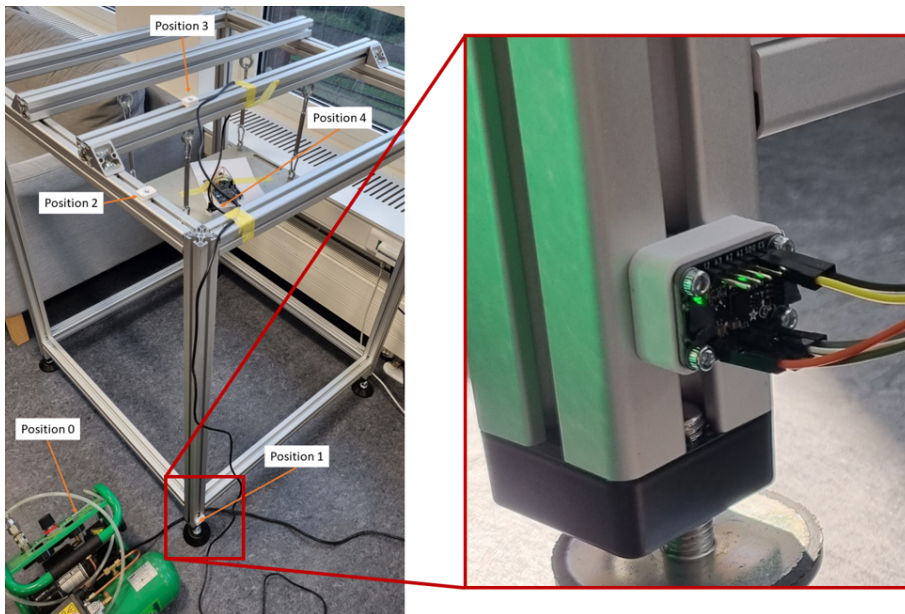


Fig. 6. Test setup and Mechanical interfaces used

For the reference measurements, the sensor is secured to the compressor frame with an M5 nut. For measurement positions on the test stand, the sensor is screwed onto a 3D-printed adapter plate which is attached to the test stand with an M6 screw. Detail shots of those interfaces can be seen on the right-hand side of Fig. 6.

Fig. 7 shows the linear spectral density of the compressor with distinct harmonics at 47 Hz and 94 Hz and high noise level on the left-hand side. On the right-hand side of Fig. 7 the compressor is switched off and only the background noise can be detected at a much lower level.

The linear spectral density as measured on the suspended test plate is shown in Fig. 8.

When comparing the linear spectral density of measurements on the test plate (Fig. 8) with those directly on the source (Fig. 7), dampening of the harmonics observed on the source is clearly shown. Overall, the current test stand setup decreases the average linear spectral density of transmitted vibrations by about one

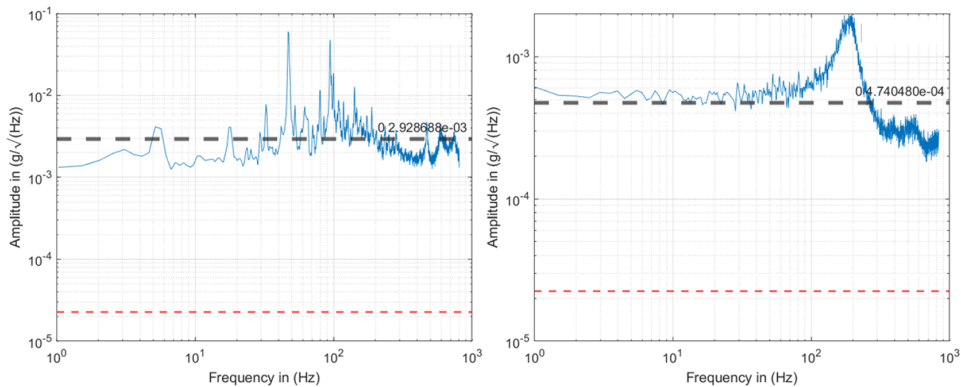


Fig. 7. Linear spectral density measured at the vibration source. Left: vibration source switched on. Right: Vibration source switched off. The red line shows the sensor noise level

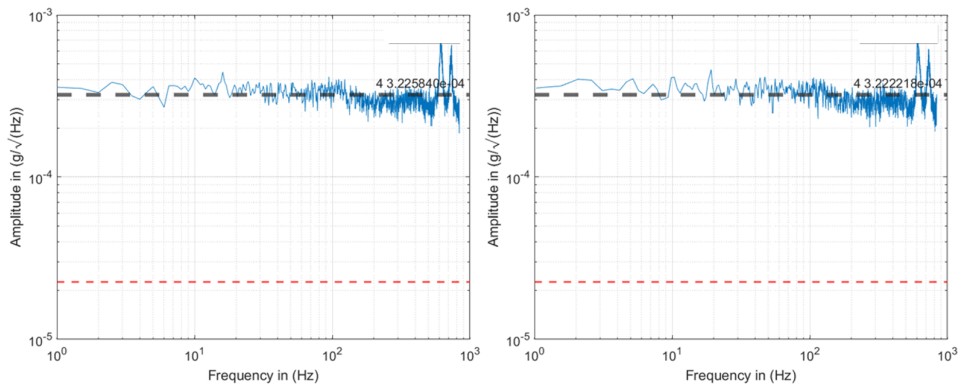


Fig. 8. Linear spectral density measured at the isolated test plate on the testbed. Left: vibration source switched on. Right: Vibration source switched off. Noise level remains low on both configurations, demonstrating the isolation features of the testbed

order of magnitude. Noise levels are decreased as well, albeit by a smaller factor. On the test plate, the effect of the compressor on the average LSD is minimal: the noise levels of Fig. 8 on the left-hand side (vibration source on) are comparable with the noise levels of the Fig. 8 on the right-hand side (vibration source off).

## 6. Next steps: Automated control and wireless implementation

### 6.1. Preliminary implementation of Active Vibration Control

The graphic in the Fig. 9 shows the test stand configurations for vibration measurements and control using the shaker and a microprocessor STM32. Two options are available, automated (option 1) and manual (option 2). Option 1 is still in the development phase, and will function as similar as described in the following.

One core of STM32 produces sine waves using its digital-to-analog converter. Next, the wave is transformed by the voltage shifter to oscillate around zero Volts and fed into the shaker driver. The frequency of the wave is automatically increased from 30 Hz to 120 Hz in 10 Hz increments. While the first core of the processor is controlling the sine wave, at the same time, the second core is responsible to read data from the accelerometers and transmit it to the user's PC where the data is saved, thus allowing real time operation. Transmission between sensor and STM32 is done through an SPI interface and transmission between STM32 and PC is realized via USB. The frequency with which data was written to the PC using this method was a maximum of 2.2 kHz. In option 2, sine waves are produced by a frequency generator and because of that the user must manually set up the frequency before each measurement. Data acquisition using STM32 in this option is done similarly to option 1, but the highest obtained frequency to save to a computer was 2.5 kHz. Using an ESP32 the only difference in data acquisition is use of UART communication and PUTTY software for data transmission to PC. In this method, the maximal obtained frequency to save to a computer was 900 Hz.

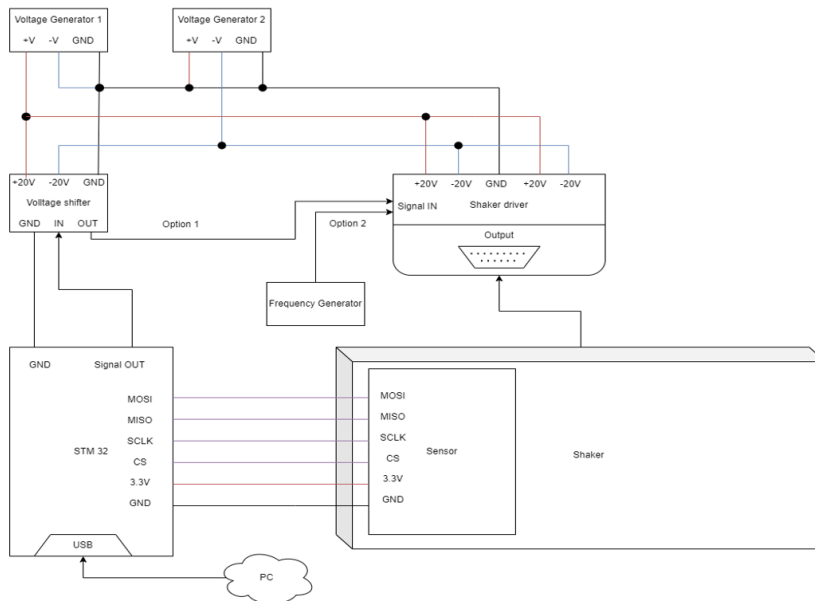


Fig. 9. Test stand electrical connections diagram for the initial implementation of automated shaker control

## 6.2. Wireless Implementation of MVMS

The wireless communication between the individual microcontrollers is implemented using the wireless nRF24L01 Transceiver Module. With these modules, up to 2 Mbps can be transmitted to any other unit in the range of 100 meters.

Additionally, each unit can communicate with up to 6 other units at the same time. These properties enable the construction of sophisticated network architectures, where many microcontrollers can send data to each other, after processing the data from the sensors. The following Fig. 10 visualizes the used basic network architecture to transmit data between microcontrollers and computers. This design shall be modified as soon as more units come into deployment.

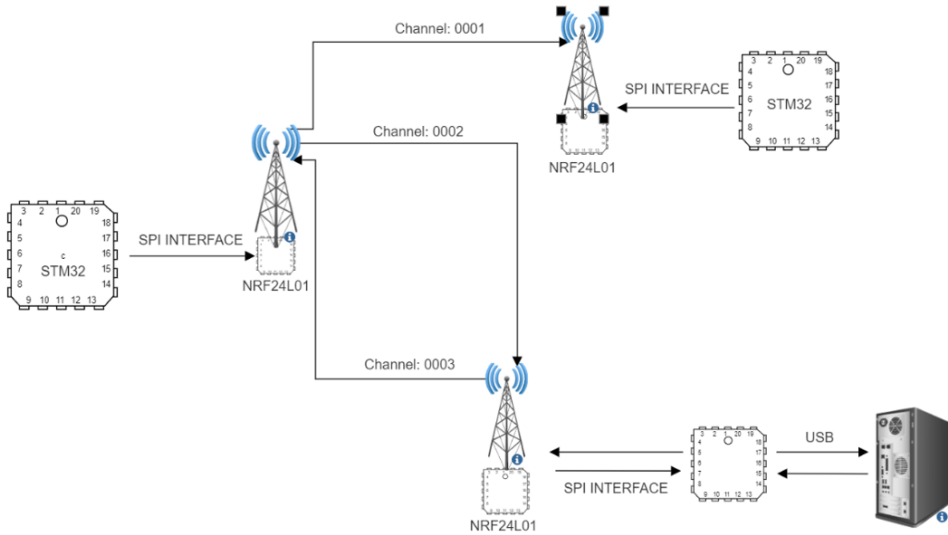


Fig. 10. Wireless setup

## 7. Conclusion and Long-Term Outlook

We have presented the VIBES microvibration project and the current status of the testbed at the IAT dedicated to develop the different elements and technologies of the project. Following an incremental approach, the first configuration of Microvibration Measurement System has been developed and characterized with specific software tools for data analysis. A dedicated shaker has been used for verification of MVMS and has been mechanically characterized, showing the needed sensitivity of the MVMS.

The mechanical testbed has been implemented and its isolation performance demonstrated, so that external background noise will not affect the measurements. This allows us to proceed to the next phase of the project: characterization of a reaction wheel on a satellite structure, both of which are already in the IAT laboratory. Next step will be the implementation of damping systems in the interface between reaction wheel and satellite structure and their characterization.

On the long-term plan, as the project is progressing, the complexity will be steadily increased. The testbed will be continuously expanded and adjusted for

different test configurations. The results from the initial exploration of different sensors and the introduction of a primitive control system to the testbed mark the beginning of a four-step plan with the eventual goal of being able to reduce and control microvibrations.

First, passive isolators will be introduced to the testbed to study their behavior. Microvibrations will be measured on all elements of the testbed in a damped and undampened configuration which will allow making an assessment whether and if yes, how extensively passive damping systems can affect the microvibrations. Using these results, improved dampers may be developed by the project team or in cooperation with research partners.

Next, the focus will shift towards active isolators. This will be done by introducing an active component to the testbed. Since passive isolators do not work efficiently against microvibrations in lower frequency ranges, the active component may provide a new scope for managing the oscillations.

Building on the gained knowledge during the previous phases, the third phase focuses on the development of an active pointing system. This entails the construction of a mechanism which actively stabilizes a given optical payload in at least two axes. In addition to compensating microvibrations and the ensuing line-of-sight error, this system will enable the compensation of quasi-static misalignment. In the final phase of the VIBES project, the developed systems will be combined in a small demonstrator (e.g., a CubeSat) to verify the functionality of the research results.

## Bibliography

- [1] ECSS. Micro-vibrations, Space Engineering: Spacecraft Mechanical Loads Analysis Handbook, ECSS-E-HB-32-26A, 2013.
- [2] A. Bronowicki. Forensic investigation of reaction wheel nutation on isolator. In *49th AIAA Structures, Structural Dynamics, and Materials Conference*, Schaumburg, IL, USA, 7-10 April 2008. doi: [10.2514/6.2008-1953](https://doi.org/10.2514/6.2008-1953).
- [3] T. Runte, Z. Perez, and M. Baro. Microvibration engineering – a key to high-performance space missions. In *70th International Astronautical Congress*, Washington, D.C., USA, 21-25 Oct. 2019.
- [4] C.J. Dennehy. A survey of reaction wheel disturbance modeling approaches for spacecraft line-of-sight jitter performance analysis. In *Proceeding of 18 European Space Mechanisms and Tribology Symposium*, Munich, Germany, 18-20 Sept. 2019.
- [5] H. Heimel. Spacewheel microvibration-sources, appearance, countermeasures. In *Proceedings of the 8th International ESA Conference on Guidance & Navigation Control Systems*, Karlove Vary, Czech Republic, 5-10 June 2011.
- [6] C. Dennehy and O.S. Alvarez-Salazar. Spacecraft micro-vibration: A survey of problems, experiences, potential solutions, and some lessons learned. Technical report, 2018.
- [7] M. Manso and M. Bezzeghoud. On-site sensor noise evaluation and detectability in low cost accelerometers. In *Proceedings of the 10th International Conference on Sensor Networks – SENSORNETS*, pages 100–106. [Online], 9-10 Febr. 2021. doi: [10.5220/0010319001000106](https://doi.org/10.5220/0010319001000106).



- 
- [8] G. Heinzel, A. Rudiger, and R. Schilling. Spectrum and spectral density estimation by the Discrete Fourier Transform (DFT), including a comprehensive list of window functions and some new flat-top windows. Technical report, 2002.
- [9] A. Wiebe. Entwicklung eines Teststandes zur Messung von Mikrovibrationen inklusive Auslegung eines Datenaufnahmesystems (Development of a test stand for measuring micro-vibrations including design of a data acquisition system). Technical report, 2021. (in German).